Electrochemical cell current requirements for toxic organic waste destruction in Ce(IV)-mediated electrochemical oxidation process

Vasily V. Kokovkin, Sang Joon Chung, Subramanian Balaji, Manickam Matheswaran and Il-Shik Moon[†]

Department of Chemical Engineering, Sunchon National University, # 315 Maegok-dong, Suncheon, Jeonnam 540-742, Korea

Abstract−The electrochemical cell for cerium oxidation and reactor for organic destruction are the most important operation units for the successful working mediated electrochemical oxidation (MEO) process. In this study, electrochemical cells with DSA electrodes of two types, single stack and double stack connected in series, were used. The performances towards the electrochemical generation of Ce(IV) in nitric acid media at 80 °C were studied. The current-voltage curves and cerium electrolysis kinetics showed the dependence on number of cell stacks needed to be connected in series for the destruction of a given quantity of organic pollutant. The presence of an optimum region for Ce(III) oxidation with a contribution of oxygen evolution, especially at low Ce(III) concentration (high conversion ratios), was found. The cells were applied for the Ce(IV) regeneration during the organic destruction. The cell and reactor processes were fitted in a simple model proposed and used to calculate the current needed in terms of Ce(III) oxidation rate and the number of cell stacks required for maintaining Ce(IV)/Ce(III) ratio at the same level during the organic destruction. This consideration was based on the kinetic model previously developed by us for the organic destruction in the MEO process.

Key words: Mediated Electrochemical Oxidation, Electrochemical Cell, Cerium, Nitric Acid, Oxygen Evolution Current, Organic Destruction

INTRODUCTION

The Mediated Electrochemical Oxidation (MEO) process has been identified as one of the promising technologies by the United Nations Environmental Program [1] for use in the developing countries for the destruction of persistent organic pollutants [2-9]. The MEO process has a major advantage over other conventional waste treatment technologies such as incineration, in that the formation of secondary pollutants is usually too small and can be easily controlled [10,11].

In the MEO process various redox pairs of different transition and inner transition metal ions have been utilized to oxidatively degrade hazardous organic species. The metal ion oxidant is electrochemically produced at the anode and subsequently used for oxidizing organic pollutants, resulting in a complete decomposition of organic materials into carbon dioxide and water in a closed environment. The oxidation of organic compounds by mediator (metal) ions, however, also accompanies the direct oxidation of organic materials at the electrode, which may lead to electrode surface poisoning and fouling. To circumvent this problem, electrochemical oxidation of metal ions is usually carried out in a separate reactor without direct contact between electrodes and pollutants. Therefore, the metal ions are continuously regenerated at an electrochemical cell and transported to the chemical reactor containing organic wastes. This cyclic usage of mediator ions makes the MEO an environmentally friendly and economical process [4,12,13].

A number of redox pairs such as Ag(I)/Ag(II) [2,3,14], Co(II)/Co(III) [2,15], Cr(II)/Cr(III), Fe(II)/Fe(III), and Ce(III)/Ce(IV) [16,17]

in an acidic medium can be used as mediator ions. Although the selectivity towards the organic materials is not general, the choice of an efficient redox system sometimes depends on the chemical composition of the waste materials. For example, the use of Ag(I)/Ag(II) in a chloride containing organic waste should be avoided due to precipitation [15].

The electrochemical cell is a core component in the MEO process. The previous works on MEO have employed commercial electrochemical cells from different manufacturers and also home-made cells [18]. Chiba [16] has utilized a plate and frame cell from Imperial Chemical Industries (Model FM-21) and Nelson et al. [19] of CerOx Corporation developed a cell of their own. Juttner et al. [12] provided an overview of various types of cells used for pollutant destruction in electrochemical approaches, but metal ion oxidation details were not available.

According to the literature cited, Ce(III) electrolysis is carried out in cells with divided anolyte and catholyte compartments by proton conducting polymeric membranes [4,20] and in undivided cells [18,21]. Usually the cells with divided compartments have higher efficiencies towards metal ion oxidation. In our study we have used our own cell with divided compartments separated by the Nafion® membrane [22-24].

It is well known that the efficiency of cerium electrolysis at an anode mainly depends on the current distribution between the Ce(III) oxidation process and water oxidation or oxygen evolution. Different anode materials and covering films influence the coulombic efficiency for Ce(III) oxidation [23]. Obviously, the most cost-effective electrodes are produced by substrate covering technologies either by electroplating or chemical vapour deposition. In our study we have used mesh titanium electrodes of DSA type coated with IrO_2 by electro-deposition.

[†]To whom correspondence should be addressed.
E-mail: ismoon@sunchon.ac.kr

When an electrochemical cell is used in the MEO process with continuous organic feeding, the main problem to be solved involves matching the Ce(IV) regeneration process in the cell to the Ce(IV) consumption due to organic destruction in the reactor. To solve this problem, we need to know the kinetic nature of organic oxidation process [24,25] in the reactor and Ce(III) oxidation (i.e. Ce(IV) regeneration) in the cell.

In our previous investigations [23,24] we have found that the optimal conditions for Ce(III) oxidation were the following. The anolyte solution was 1 M cerium nitrate in 3 M nitric acid, catholyte was 4 M HNO_3, temperature of the solution was 80 °C and a constant current of 10 A. In this paper, we describe the performance of homemade electrochemical cells assembled in single stack and double stack configurations. A model is proposed to calculate the current consumption during the organic destruction and the number of cell stacks of specified size required for maintaining Ce(IV)/Ce(III) ratio at the same level. This model is based on a kinetic model for continuous mode of organic destruction previously developed and reported by us [24,25].

Ethylenediaminetetra acetic acid (EDTA) is an efficient chelating agent used in many different industrial applications for complexing metal ions. It is also an important decontaminating agent in the nuclear industry. When radioactive wastes are treated with EDTA, it forms strong and highly mobile radioactive metal complexes. These complexes when released into the environment pose a potential threat to humans [26]. Although EDTA by itself is relatively harmless to human beings, it may produce deleterious effects by increasing metal distributions to the surrounding environment through enhanced mobility of metal-EDTA complexes [27,28]. The presence of EDTA in waste water can increase the level of lead and zinc as much as 200% [29]. In the US the EDTA concentrations in waste water effluent discharge have been reported at 1-72 μg/L. Therefore, degradation of EDTA becomes important and has been attempted by the MEO process.

EXPERIMENTAL

A schematic diagram of the MEO system used for this study is shown in Fig. 1. The system consisted of an anolyte, catholyte, and chemical reactors each with a capacity of 1.5 L, respectively. The anolyte and catholyte solutions were circulated through the cell with a ceramic pump (Pan World magnet pump, Model NH-40PX-N).
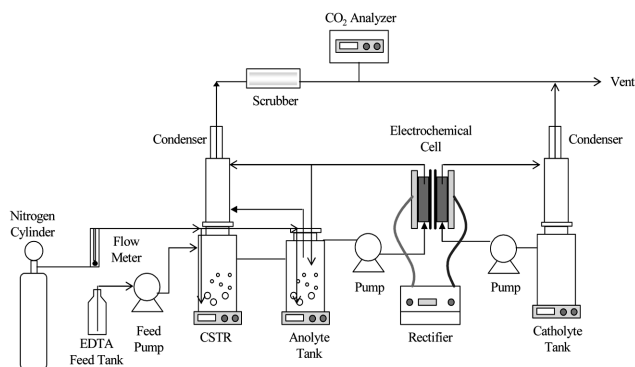

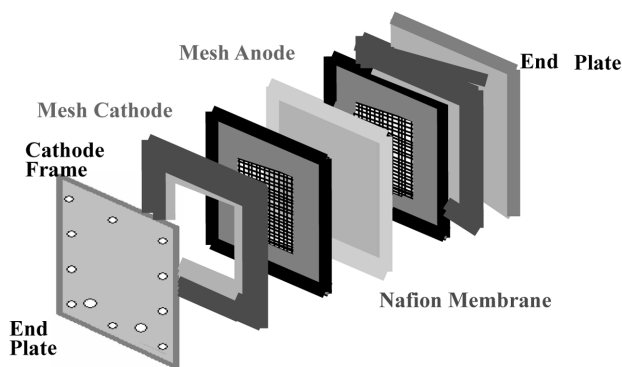
Fig. 1. Schematic diagram of MEO process setup.

Fig. 2. Section view of the electrochemical cell.

The mediator solution oxidized at the cell was transported to the chemical reactor equipped with a scrubber and an online CO_2 analyzer to estimate the amount of CO_2 produced during the oxidation of organic wastes. The organic to be destroyed was fed to the chemical reactor from the feed tank. The catholyte part was also provided with a gas scrubber to capture the nitrous vapors produced.

Single and double stack electrochemical cells were used. The single stack electrochemical cell (Fig. 2) consisted of a pair of anode and cathode separated by a Nafion®324 proton exchange membrane (Dupont, USA). The double stack cell consisted of two single stack cells assembled in one unit and electrically connected in series. The electrodes in both cells utilized were IrO_2-coated on Ti mesh substrate (area: 140 cm^2). A fluoro-polymer sheet (Viton®) possessing excellent chemical and heat resistance was used as a separator.

The anolyte solution was prepared by dissolving 1 M cerium(III) nitrate in 3 M nitric acid. The catholyte was 4 M nitric acid solution. The temperature of the solution was controlled by heating mantle and air was purged continuously through the catholyte solution to convert nitrous acid, produced by reduction at the cathode, to nitric acid. A constant current (galvanostatic mode) or voltage (potentiostatic mode) was provided to the electrochemical cell by a constant DC voltage supply (Korea Switching, 10 V, 100 A). During the reaction, concentration changes of Ce(IV) were monitored by measuring the redox potential with a Pt-Ag/AgCl combined electrode with an Orion pH/ISE meter (Model No. 720 A, Orion Co. Ltd., USA) and cross-checked by titration with ferrous (II) sulfate [31]. The concentration of oxygen was measured by an infra red analyzer (Environmental Instruments, Anagas CD 98). The cell operating conditions were found on the basis of current-voltage curves (I-V curves), kinetics of Ce(III) oxidation and oxygen evolution at galvanostatic and potentiostatic regimes and compared based on the coulombic efficiency.

During the destruction of an organic material, nitrogen was passed to carry carbon dioxide produced from the reactor to the CO_2 analyzer. The extent of destruction was calculated from the amount of CO_2 evolved. The direct measurement of amounts of carbon remaining in the solution was also performed using a total organic carbon analyzer (Shimadzu TOC 5000A). The error of estimation lies within 2-3% in all determinations.

RESULTS AND DISCUSSION

1. Electrochemical Cell Characteristics

The current-voltage curves (I-V curves) for both cells were measured at anode polarizing potentials. Fig. 3 compares I-V curves between single stack and double stack cells at 1 M Ce(III) in 3 M HNO₃ at 80 °C, which corresponds to the initial electrolysis stage. The shape of the curves reflects the complex mechanism of cerium oxidation and oxygen evolution processes. This can be compared to the I-V curve for 3 M HNO₃ solution. The process in the case of pure nitric acid can be fully attributed to the water oxidation. From the comparison one can find some cerium oxidation current "window" in the range 1.75-3.5 V for single stack cell and 3.2-6 V for double stack cell (the curves for cerium containing solutions). From the shape of the curves, it is hard to find the point from where oxygen evolution process is beginning and suppressing cerium oxidation. This result is in agreement with previous observations as for divided [20] and

undivided [18,21] cells.

The potential window of 1.75-3.5 V corresponds to the current region 5-45 A for single stack cell and 3.2-6 V to 4-40 A for double stack cell. This difference is nearly 2 times and the increase in voltage can be attributed to the internal resistance of the cells. The current and potential regions mentioned were used for searching the optimal conditions in galvanostatic and potentiostatic cell operating modes. As a parameter for optimization, the coulombic efficiency of Ce(III) oxidation during the electrolysis was chosen. One of the data sets for coulombic efficiency versus current applied in the single stack cell for 90% conversion during galvanostatic electrolysis is presented in Fig. 4. These data clearly show that some optimal current region is 8-10 A. Therefore, in all further galvanostatic experiments, 10 A current was chosen for the cell operation as in a previous investigation [23]. The same result was also obtained for the double stack cell. The application of potentiostatic regime for both cells showed that optimal conditions for cells operation were 2.5 V
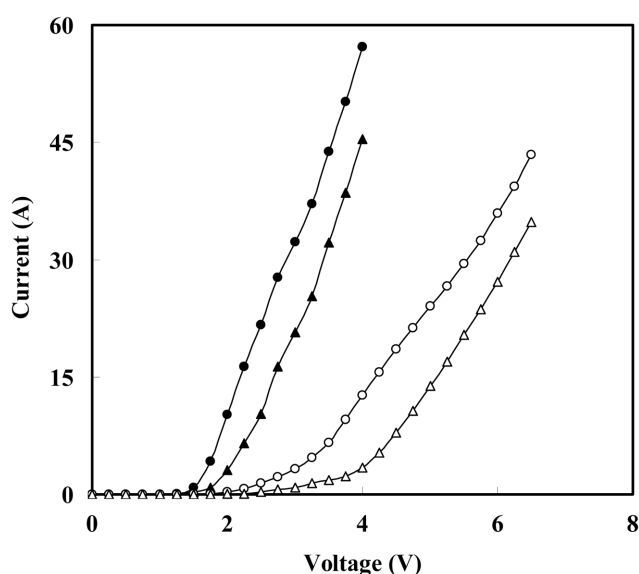

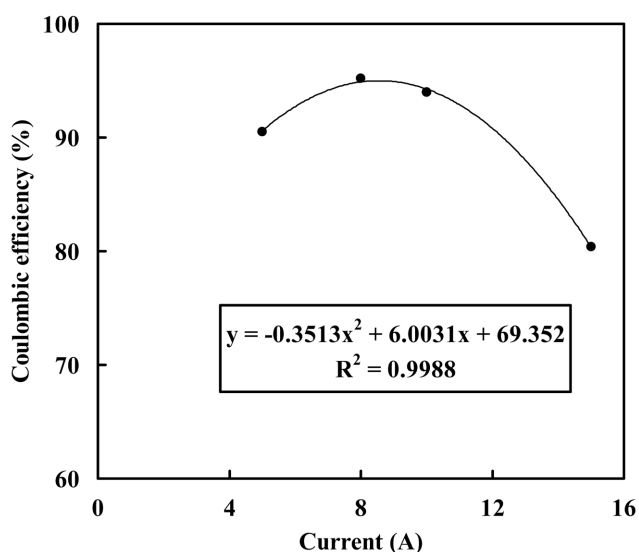Fig. 3. Current-voltage curves of single (a) and double (b) cells at 80 °C.

Fig. 4. The coulombic efficiency for 90% conversion Ce(III) to Ce (IV) on current applied for galvanostatic electrolysis.

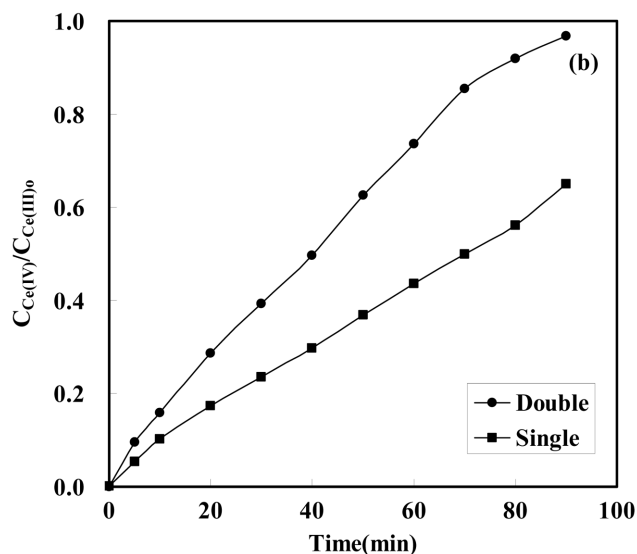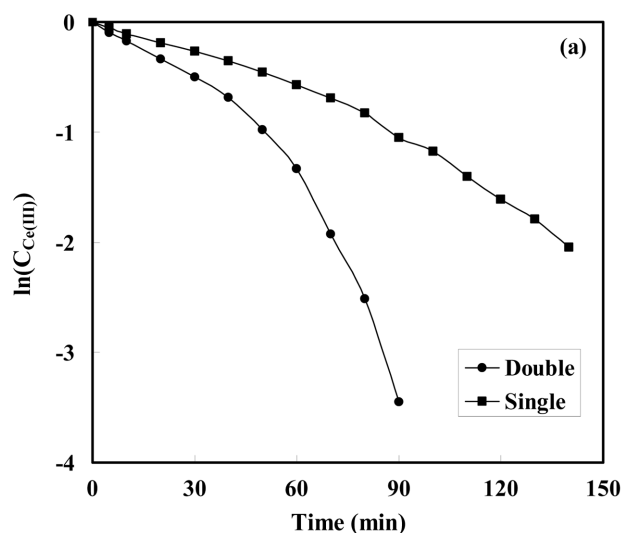$$y = -0.3513x^2 + 6.0031x + 69.352$$
$$R^2 = 0.9988$$

Fig. 5. Ce(III) oxidation kinetics (a) and extent of conversion (b) during electrolysis for single and double cells at 10 A galvanostatic regime at 80 °C; the volume of anolyte and catholyte solutions 1,000 cm³.

for the single stack and 5 V for the double stack cell.

The difference between the cells can be found only in the intensity of Ce(IV) production. This is important for the MEO process where Ce(IV) consumed should be regenerated in a short duration. In Fig. 5, the kinetics of cerium oxidation is presented for both types of cell. In the figure the dependence of time vs $\ln C C e_{(III)}$ is shown. The linearity of dependences for both cells is extended up to $\ln C C e_{(III)} = -1.5$. It corresponds to 70-80% of conversion to Ce(IV). This observation is in accordance with the diffusional nature of the cerium oxidation process [20,21]. From the slope of the dependence, using limiting current approach and total MEO solution volume, the mass transfer coefficient (K_L) can be calculated. It is 0.28 cm^3 s^{-1} for the single stack cell and 0.48 cm^3 s^{-1} for the double stack cell. A difference in K_L values nearly two times between the cells was expected because of the difference in surface area of the cells. These values will be used in later discussions.

The flow rate of the solution is a critical parameter when the process is controlled by the diffusion. In our case, a constant solution flow rate of 4-5 L min^{-1} was used. It corresponds to the solution velocity near electrode surface of 0.12-0.16 m s^{-1}. According to Ralph et al. [30] above the solution velocity of 0.16 m s^{-1} the rate of increase of mass transfer coefficients is reduced. Therefore, this region can be considered as the high turbulent region and with maximum mass transfer rate. After reaching 70-80% conversion, cerium oxidation is substantially affected by water oxidation and cerium mass transfer coefficients were changed.

In order to understand the role of water oxidation during the cell operation, oxygen evolution was measured during cerium oxidation. These data were split into individual current values for cerium oxidation and oxygen evolution. Fig. 6 shows the dependence $CCe_{(III)}$ vs I/I(tot). When the electrolysis begins and the Ce(III) concentration is high (near 0.8-1.0 M), partial current for cerium oxidation is equal to unity. The oxygen current is nearly zero in this range. It starts to increase only after 0.7 M of Ce(III) and becomes substan-

tial (higher than 50%) after Ce(III) decreases to less than 0.2 M. It is in accordance with the change of linear dependence for cerium oxidation kinetics. These values were used in the calculations based on a simple model for fitting the currents of Ce(III) oxidation in a cell and Ce(IV) consumption in the reactor during the organic destruction.

2. Organic Destruction in MEO Process

Usually after oxidant solution was prepared in the cell, organic was fed and destructed in the reactor. In most of the experiments organic feeding time was at least 30 minutes, but the final destruction product, i.e., CO$_2$, was monitored for much longer durations to ensure the complete destruction of the remaining organic in the liquid phase. During the organic destruction, the cell was working at 10 A constant current supply for maintaining Ce(IV) concentration nearly at the same level.

In our experiments we previously studied the oxidation of EDTA, aniline, phenol and its oxidative derivatives like hydroquinone, oxalic acid, maleic acid etc. [23-25]. As an example for EDTA, the stoichiometry of the oxidation reaction can be represented by the following formal equation verified by Ce(IV) titration and TOC determination.

$$C_{10}H_{14}O_8N_2Na_2 + 40Ce(IV) + 12\,H_2O$$
$$\rightarrow 10\,CO_2 + 40\,Ce(III) + 38\,H^+ + N_2 + 2Na^+ \tag{1}$$

According to our experimental data, CO$_2$ formation kinetics obeyed the first order reaction rate for most organics studied. In this way, CO$_2$ evolution can be considered as a result of a simple one step reaction mechanism and the reactants are expressed in terms of total organic carbon content. The total organic carbon content really reflects the concentration of all organics remaining in the MEO solution, e.g., residual EDTA and different intermediates formed [23-25]. Therefore, for forward reaction rate we can write:

$$v = -\frac{dC_{carbon}(t)}{dt} = kC_{carbon}(t) = \frac{dX(t)}{dt} = k(C_o - X(t)) \tag{2}$$

As previously mentioned, in our continuous feeding mode experiments the experimental procedure consists of two parts. In the first, the organic is added at a particular time with simultaneous destruction, and in the second, after the organic feeding is stopped, destruction only takes place. The CO$_2$ evolution pattern during EDTA destruction is shown in Fig. 7a for 2.5% EDTA (flow rate 3 ml min^{-1} during 30 min), at 80 °C with 0.95 M Ce(IV) and 3 M nitric acid as the mediator solution.

In the continuous process for finding the k value it is necessary to find the balance between the amounts of organic added and the CO$_2$ produced. For the first part of the curve, we used a differential method in which the total time of organic addition was divided into small intervals, e.g., one min within which organic was considered as adding one portion. Calculation of the remaining organic carbon was done by using summation by geometrical progression, e.g., for the mth step of addition it is equal to:

$$C_{carbon} = \frac{\Delta C_{carbon}(1 - \exp(-km\Delta t))}{1 - \exp(-k\Delta t)} \tag{3}$$

After organic feeding is stopped, the second part of the curve should obey usual batch destruction kinetics. The CO$_2$ evolved was calculated at every step of organic addition as the difference between the total organic carbon added and remaining. Since k is the only param-
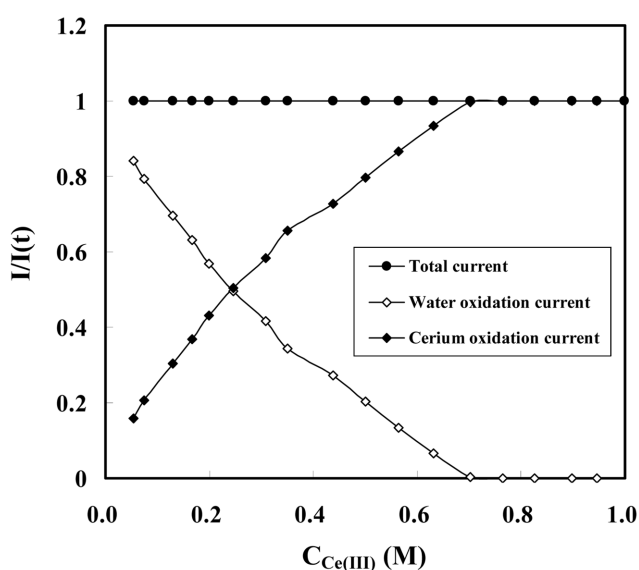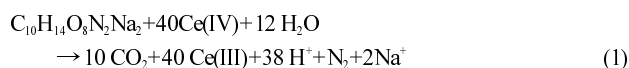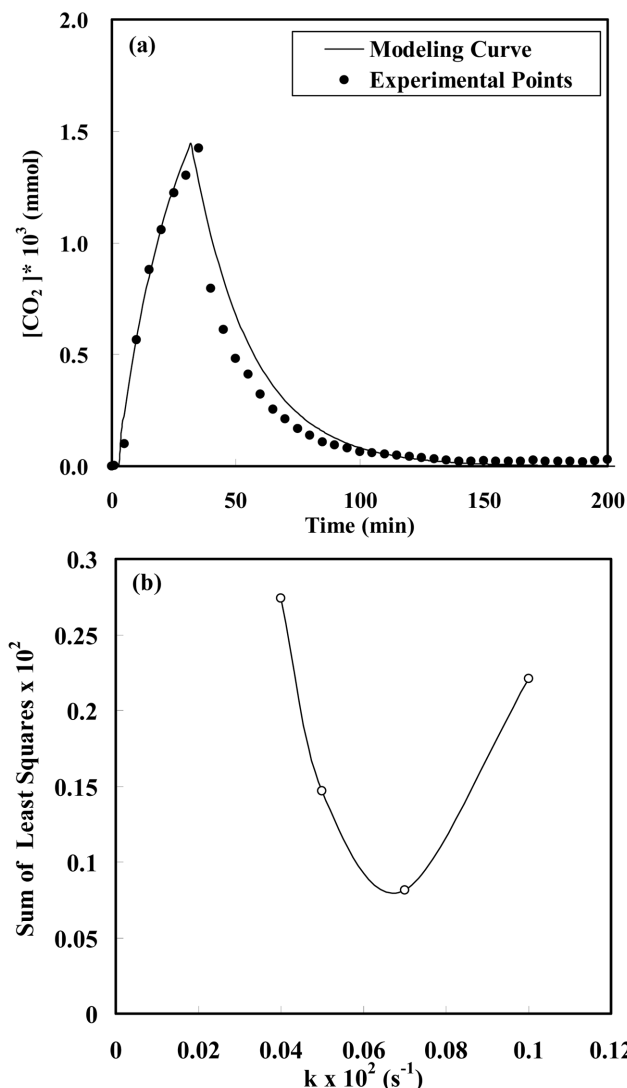

Fig. 6. The relationship between total current and its constituents including Ce(III) and water oxidation during galvanostatic electrolysis at 10 A at 80 °C for single cell.

Fig. 7. Modeling curve for EDTA destruction and data fitting: the best fit between modeling curve and experimental data (a); least square curve (b).

Fig. 8. Modeling curves for three destruction processes with k= 3.5×10^{-4}; 7.0×10^{-4} and 1.2×10^{-3} s^{-1} at 3 ml min^{-1} feeding rate of 2.5% EDTA (a); experimental curve for CO_2 evolution during 2.5% EDTA destruction at 80 °C (b).

eter in calculations, a simple procedure is proposed to find it from the experimental data. Setting k values in the appropriate range, several modeling curves can be drawn for the given organic concentration and flow rate. The sum of the squares of the difference between the experimental and modeling data was calculated for each of them according to the least squares method (LSM). The plot of the sums vs. k is presented in Fig. 7b. The k=0.0007 s^{-1} value with minimum difference by LSM was chosen as the closest one to the experiment for the conditions stated above.

The data set presented in Fig. 7 corresponds to the experimental conditions of 30 min feeding time. In real applications, however, long time feeding is needed (hours, days etc.). It means that the MEO solution should not accumulate the organic substances. The organics should be completely and constantly destructed upon feeding. Therefore, in the destruction process, some steady state regime should come into existence. The proposed model for remaining organic calculation was tested for much longer time periods.

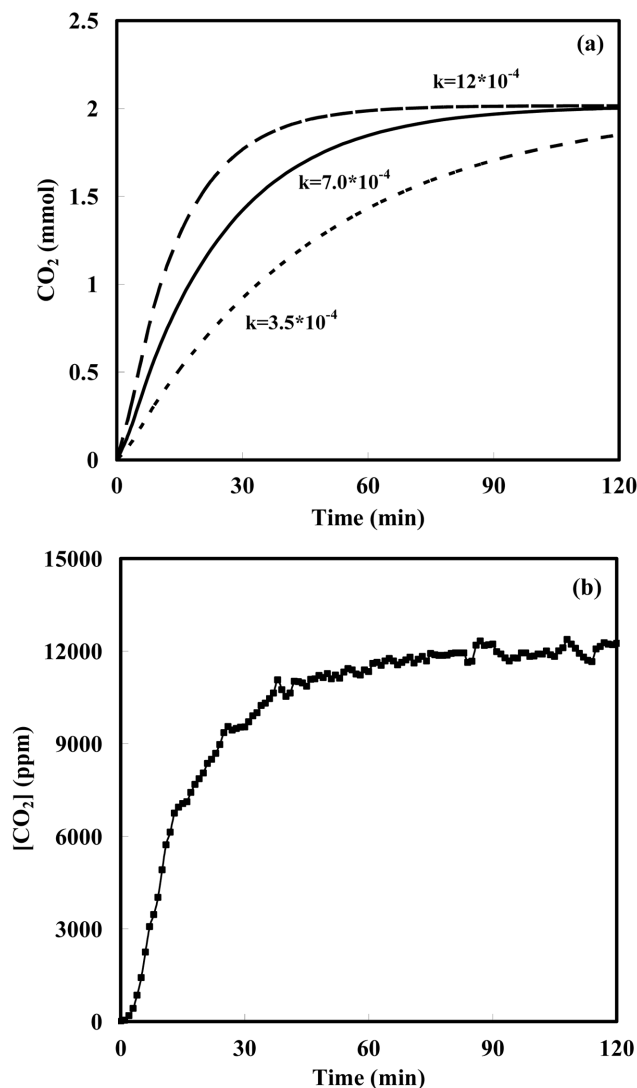Fig. 8a presents the modeling curves for long time feeding (2.5

hr) for three processes of CO_2 evolution, having k values of 3.5×10^{-4}; 7.0×10^{-4} and 1.2×10^{-3} s^{-1} at 3 ml min^{-1} feeding rate of 2.5% EDTA. As can be seen in the figure, the steady state really comes after 40 min for the process with k=1.2×10^{-3} and after 100 min with k=7.0×10^{-4}. However, for k=3.5×10^{-4}, the steady state was not reached up to 2.5 hr. This process may need much more time for reaching a steady state. It can be noticed here that the steady state attainment of CO_2 evolution does not depend on values of kinetic constants. These findings led us to conclude that the proposed model satisfactorily predicted the steady state condition for organic feeding and simultaneous destruction. Subsequent experimental results conformed to the model predictions. The experimental curve for 2 hr organic feeding is presented in Fig. 8b.

3. Calculations of the Cell Current Need in the MEO Destruction Process

The basic idea used for calculating the current needed to maintain Ce(IV) concentration at the same level in the MEO destruc-

tion process was the following. The rate of cerium oxidation in the cell should be the same and should match with the rate of Ce(IV) reduction in reactor. Using Eqs. (1) and (2) for EDTA we get,

$$v_{carbon} = \frac{p}{q} v_{Ce(IV)} \qquad (4)$$

where $v_{carbon} = -dC_{carbon}/dt$ and $v_{Ce(IV)} = -dC_{Ce(IV)}/dt$ are the rates of organic carbon oxidation and Ce(IV) reduction. Additionally, for EDTA destruction p=10 and q=40.

The rate of Ce(III) oxidation in the electrochemical cell is equal to

$$v_{Ce(III)} = \frac{dQ}{n_e F V dt} = \frac{I}{n_e F V} \qquad (5)$$

Using the Eqs. (4) and (5), we find that cerium oxidation current will be

$$I = n_e \frac{q}{p} F k C_{carbon} V \qquad (6)$$

Note, that this is only cerium oxidation current. If we need total current we should consider the water oxidation process.

Our calculations show that the current needed for cerium regeneration at steady state does not depend on the rate constant value. It is the same for processes with k values differing more than three times from 1.2×10^{-3} to 3.5×10^{-4}. But, it is in linear dependence on concentration and feeding rate of organic. So, if organic concentration increases two times (from 2.5 to 5.0%), then the steady state current also increases two times (compare 10.5 and 21.0 A calculated using Eq. (6)). Note, that the current needed for destruction of EDTA at 2.5% concentration and 3 ml min⁻¹ has nearly the same value as the optimal current needed for a single stack cell. But, it is total current. From the rate of organic destruction, cerium oxidation current only was calculated, and at conversion rates less than 80% total current approximately was equal to cerium oxidation current. Using our experimental results on Ce(III) oxidation with electrochemical cells it is possible to calculate the level of Ce(III) concentration during the process of organic destruction by the following equation:

$$C = \frac{I}{n_e F K_L} \qquad (7)$$

Table 1. Estimation of number of cells required for keeping Ce(III) oxidation at definite K_L values at constant cell current supply of 10 A

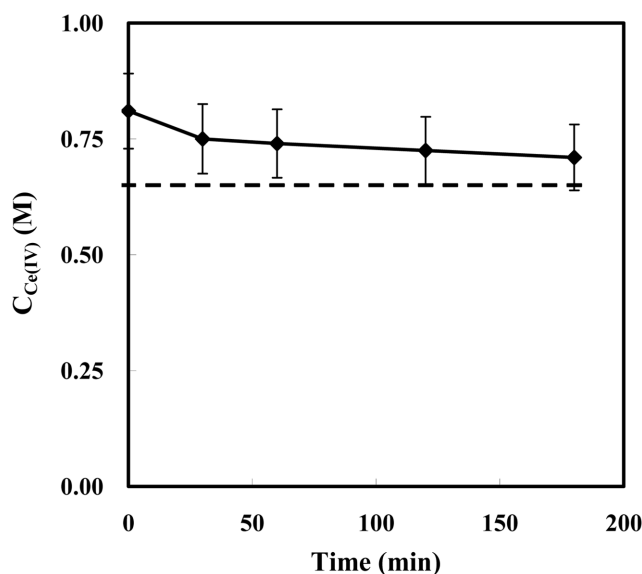| S. No.	Ce(III), mole/dm³	Ce(IV)	K_L, cm³/s	No of cells
1	0.05	0.95	2.18	7.8
2	0.1	0.9	1.09	3.9
3	0.2	0.8	0.54	1.9
4	0.23	0.77	0.48	1.71 (double)
5	0.3	0.7	0.36	1.2
6	0.38	0.62	0.28	1 (single)
7	0.4	0.6	0.26	0.9
8	0.5	0.5	0.21	0.75
9	0.6	0.4	0.17	0.6
10	0.7	0.3	0.15	0.53

Fig. 9. Experimental results of Ce(IV) monitoring (solid line) for 3 hr of EDTA feeding with destruction in MEO process (EDTA feeding solution 2.5% and 3 ml min⁻¹) and calculated steady state Ce(IV) concentration using the model (dotted line).

The result of calculation of Ce(III) and Ce(IV) for EDTA (concentration 2.5% and flow rate 3 ml min⁻¹) is presented in the sixth row of Table 1. It is necessary to point out that this result corresponds to the single stack cell, and 10 A current is cerium oxidation current. The total current can be found from the dependences similar to those presented in Fig. 6. The value of Ce(III) concentration corresponds to 0.38 M and Ce(IV) to 0.62 M. Experimental results for Ce(IV) monitoring up to 3 hr of EDTA destruction in MEO process are presented in Fig. 9. As we predicted, Ce(IV) concentration is very close to experimental data within 10% error bars. This means that within assumptions made in calculations we get a suitable result from the actual experimental MEO process.

In Table 1 the data calculated with Eq. (7) are also presented for Ce(III) concentrations as lower and higher than for single cell capacity. Hence, one can conclude that for keeping Ce(III) concentration at low levels and at the same time Ce(IV) at high levels, it is necessary to have K_L values higher than we have in our single cell. In this case double stack cell can be used. The data calculated for double cell are presented in the fourth row of Table 1. According to the calculations it is not exactly equal to 2 but somewhat lower because of a difference in flow rate regimes and electrode characteristics.

In our calculations, it was found that nearly eight cells are needed to keep the concentration of Ce(III) at the level 0.05 M. The validity of our model can be expected to be in good agreement only if cerium conversion is less than 80%. When conversion rates are higher than 80%, mass transfer coefficients substantially change because of water oxidation. According to Fig. 5, mass transfer coefficients are increased in this conversion region. But the kinetic consideration for current calculations is more complicated and now it is under investigation.

Finally, we conclude that our calculations based on simple considerations of the diffusional nature of Ce(III) oxidation current (in

a region less than 80% conversion) in the cell process and organic destruction as a simple one-step reaction give us the possibility to predict the number of cells required for a given quantity of organic waste. The model, although approximate, may serve as a useful tool for engineering design applications of the MEO process.

CONCLUSIONS

1. Electrochemical cells of single stack and double stack type were constructed and their performances were studied for the electrochemical oxidation of Ce(III) in 3 M HNO_3 with and without continuous organic feeding. It was found that the range of 8-10 A current supply in galvanostatic mode is optimal in terms of current efficiency for both cell types. In potentiostatic mode optimal conditions were 2.5 V for single cell and 5 V for double cell. Ce(III) electrolysis data showed substantial role of diffusional current up to 80% conversion ratios.

2. Kinetics of CO_2 evolution and Ce(IV) consumption during destruction of EDTA in continuous MEO process was studied. Using a simple first order kinetic model approach and differential method for reactant and product balance calculations on the basis of summation of geometric progression, reaction constants were estimated. It was shown that during long-term operation the process attains steady state, which does not depend on the value of reaction constants but mainly on concentration and feeding rate of organic.

3. A simple model was proposed to calculate the steady state current for organic destruction by Ce(IV)-MEO process and the number of electrochemical cells required (of specific size used) for Ce(III) oxidation based on a diffusional current approach and continuous organic destruction model was estimated. The obtained results will be used for process scale up.

ACKNOWLEDGMENTS

NOMENCLATURE

$C_{Ce(III)}$: concentration of cerium(III) [kmole m^{-3}]
$C_{Ce(IV)}$: concentration of cerium(IV) [kmole m^{-3}]
C_{carbon} : concentration of organic carbon [kmole m^{-3}]
F : faraday's constant [Coulomb $mole^{-1}$]
I : partial current for cerium(III) oxidation or water oxidation [A]
I(tot) : total current in the cell [A]

K_L : mass transfer coefficient [m^3 s^{-1}]
k : first order reaction rate constant [s^{-1}]
p : stoichiometry of carbon
Q : electrical charge [Coulomb]
q : stoichiometric coefficient for cerium in formal reaction for organic oxidation
t : time [s]
V : volume of the MEO solution [m^3]
X : concentration of the product for the reaction of organic destruction like CO_2 [kmole m^{-3}]

Greek Letters

Δ : dimensionless difference operator
ν : reaction rate [mole·m^{-3}·s^{-1}]

Subscripts

o : zero time
e : electron

REFERENCES

1. GEF, *On review of emerging innovative technologies for the destruction and decontamination of POPs and the identification of promising technologies for use in developing countries,* Report of the United Nations Environmental Programme for 2004, January 15 (2004).
2. J. Bringmann, K. Ebert, U. Galla and H. Schmieder, *J. Appl. Electrochem.,* **25**, 846 (1995).
3. J. C. Farmer, *Environmental oriented electrochemistry,* Elsevier Science Publishers, Amsterdam (1992).
4. J. C. Farmer, F. T. Wang, R. A. Hawley-Fedder, P. R. Lewis, L. J. Summers and L. Foiles, *J. Electrochem. Soc.,* **139**, 654 (1992).
5. P. M. Dhooge, D. E. Stilwell and S. M. Park, *J. Electrochem. Soc.,* **129**, 1719 (1982).
6. K. Kramer, P. M. Robertson and N. Ibl, *J. Appl. Electrochem.,* **10**, 29 (1980).
7. N. J. Nelson, *Handbook of mixed waste management technology,* CRC Publishing, Boca Raton, FL (2001).
8. D. F. Steele, *Platinum Met. Rev.,* **34**, 10 (1990).
9. D. F. Steele, D. Richardson, D. R. Craig, J. D. Quinn and P. Page, *Electrochemistry for a cleaner environment,* The Electrosynthesis company, East Amherst, NY (1992).
10. T. Tzedakis and A. Savall, *Chem. Eng. Sci.,* **46**, 2269 (1991).
11. J. Varela, S. Oberg, T. M. Neustedter and N. Nelson, *Environ. Prog.,* **20**, 261 (2001).
12. K. Juttner, U. Galla and H. Schmieder, *Electrochim. Acta,* **45**, 2575 (2000).
13. S. J. Chung, S. Balaji, M. Matheswaran, T. Ramesh and I. S. Moon, *Water Sci. Technol.,* **55**, 261 (2007).
14. M. Matheswaran, S. Balaji, S. J. Chung and I. S. Moon, *J. Ind. Eng. Chem.,* **13**, 231 (2007).
15. Y. H. Chung and S. M. Park, *J. Appl. Electrochem.,* **30**, 685 (2000).
16. Z. Chiba, *Mediated electrochemical oxidation of mixed wastes,* Lawrence Livermore National Laboratory, Livermore, CA, UCRL-JC-112669, April (1993).
17. Y. Wei, B. Fang, T. Arai and M. Kumagai, *J. Appl. Electrochem.,* **35**, 561 (2005).
18. T. Raju and C. Ahmed Basha, *Chem. Eng. J.,* **114**, 55 (2005).

19. N. Nelson, *Platinum Met. Rev.*, **46**, 18 (2002).
20. R. M. Spotnitz, R. P. Kreh, J. T. Lundquist and P. J. Press, *J. Appl. Electrochem.*, **20**, 209 (1990).
21. T. A. Sedneva, *Russian J. Appl. Chem.*, **78**, 907 (2005).
22. I. S. Moon, Korea Patent 10-2005-0045983 (2005).
23. S. Balaji, S. J. Chung, T. Ramesh and I. S. Moon, *Chem. Eng. J.*, **126**, 51 (2007).
24. S. Balaji, V. V. Kokovkin, S. J. Chung and I. S. Moon, *Water Res.*, **41**, 1423 (2007).
25. J. W. Lee, S. J. Chung, S. Balaji, V. V. Kokovkin and I. S. Moon, *Chemosphere*, **68**, 1067 (2007).
26. J. Gardiner, *Water Res.*, **10**, 507 (1976).
27. J. L. Means, D. A. Crerar and J. O. Duguid, *Science*, **200**, 1477 (1978).
28. J. Cleveland and T. Rees, *Science*, **212**, 1506 (1981).
29. A. C. Alder, H. Siegrist, W. Gujier and W. Giger, *Water Res.*, **24**, 733 (1990).
30. T. R. Ralph, M. L. Hitchman, J. P. Millington and F. C. Walsh, *Electrochim. Acta*, **41**, 591 (1996).
31. M. Matheswaran, S. Balaji, S. J. Chung and I. S. Moon, *Chemosphere*, **69**, 325 (2007).